Results in Control and Optimization 18 (2025) 100539

Contents lists available at ScienceDirect

Results in Control and Optimization

journal homepage: www.elsevier.com/locate/rico

Frequency regulation of two-area thermal and photovoltaic power system via flood algorithm

Serdar Ekinci [a], Davut Izci [b,h], Cebrail Turkeri [a], Aseel Smerat [c,d,g], Absalom E. Ezugwu [e], Laith Abualigah [f,*]

[a] Department of Computer Engineering, Batman University, Turkey
[b] Department of Electrical and Electronics Engineering, Bursa Uludag University, 16059, Bursa, Turkey
[c] Faculty of Educational Sciences, Al-Ahliyya Amman University, Amman 19328, Jordan
[d] Centre for Research Impact & Outcome, Chitkara University Institute of Engineering and Technology, Chitkara University, Rajpura, 140401, Punjab, India
[e] Unit for Data Science and Computing, North-West University, 11 Hofman Street, Potchefstroom 2520, South Africa
[f] Computer Science Department, Al al-Bayt University, Mafraq 25113, Jordan
[g] Computer Technologies Engineering, Mazaya University College, Nasiriyah, Iraq
[h] Applied Science Research Center, Applied Science Private University, Amman 11931, Jordan

ARTICLE INFO

Keywords:
Load frequency control
Renewable energy
Flood algorithm
PI controller design
Meta-heuristic optimization

ABSTRACT

Frequency regulation is critical for maintaining balance between supply and demand in interconnected power systems, ensuring grid stability and preventing disruptions. This becomes increasingly important with the integration of renewable energy sources, such as photovoltaic (PV) units, which introduce variability and complexity into power systems. In this regards, this study presents a novel approach to frequency regulation in a two-area interconnected power system comprising thermal and PV units. A Proportional-Integral (PI) controller is designed, and its parameters are optimally tuned using the flood algorithm (FLA). The innovative use of the FLA ensures robust performance and efficient frequency stabilization under varying operational conditions. The implementation details of the FLA-tuned PI controller are provided, and its performance is rigorously compared with PI controllers tuned using several state-of-the-art optimization techniques. These include sea horse optimization, salp swarm algorithm, whale optimization algorithm, shuffled frog-leaping algorithm, and firefly algorithm. The comparative analysis is based on numerical results of performance metrics, demonstrating the robustness and effectiveness of each tuning method. Performance indices, including maximum overshoot, settling time and steady-state error are used to evaluate the robustness of the designed PI controllers. The frequency variations for the two-area thermal and PV power system are analyzed post-optimization, highlighting the superiority of the FLA-based PI controller in maintaining system stability under various operational conditions. The proposed FLA-based PI controller achieved a reduction in maximum overshoot by 28.3 %, a decrease in settling time by 23.4 %, and an improvement in steady-state error by 15.7 % compared to the next best-performing optimization method. These results demonstrate the significant advantages of the FLA in optimizing frequency regulation.

* Corresponding author.
E-mail addresses: davutizci@gmail.com (D. Izci), aligah.2020@gmail.com (L. Abualigah).

https://doi.org/10.1016/j.rico.2025.100539
Received 20 September 2024; Received in revised form 29 January 2025; Accepted 16 February 2025
Available online 20 February 2025
2666-7207/© 2025 The Authors. Published by Elsevier B.V. This is an open access article under the CC BY-NC-ND license (http://creativecommons.org/licenses/by-nc-nd/4.0/).

1. Introduction

The increasing integration of renewable energy sources, particularly photovoltaic (PV) systems, into power grids has introduced new challenges in maintaining grid stability and reliability. Among these challenges, frequency regulation remains a critical aspect, especially in multi-area power systems where different regions or "areas" are interconnected [1,2]. In a two-area thermal and PV power system, effective frequency regulation ensures the balance between supply and demand, maintaining the nominal frequency and preventing system instability [3]. Integrating PV units into power systems poses unique challenges due to their intermittent and non-dispatchable nature. Unlike traditional thermal power plants, which provide consistent and controllable energy output, PV systems are highly dependent on weather conditions such as solar irradiance. This variability can result in sudden frequency deviations, making it more difficult to maintain grid stability. Additionally, PV units lack inherent inertia, which is critical for dampening frequency fluctuations. These characteristics necessitate the development of advanced control strategies to ensure reliable frequency regulation in systems with significant PV penetration.

In traditional power systems, frequency regulation is primarily managed by thermal power plants through governor control mechanisms [4]. However, the inclusion of PV power introduces variability due to the intermittent nature of solar energy, which necessitates advanced control strategies to manage the frequency deviations effectively. In a two-area system, each area may have distinct characteristics and generation sources, making coordinated control essential for overall system stability. Frequency regulation in a two-area thermal and PV power system involves controlling the power output of generators to match the load demand while minimizing frequency deviations. This is particularly important because frequency deviations can lead to power quality issues, equipment damage, and even system blackouts [5]. In such a system, the control strategy must address the dynamic interactions between the thermal and PV generation units, considering the inertia of thermal plants and the fast response characteristics of PV systems [6].

To address the load-frequency regulation for power system, various control strategies have been developed, including the artificial neural network controllers [7] and the fuzzy logic controllers [2,8]. Additionally, robust control methods like linear quadratic gaussian control (LQR) [9], H-infinity [10], and others have been applied to achieve improved system performance. These methods offer robustness against uncertainties and disturbances but often come with increased complexity and computational requirements.

In contrast, the proportional-integral (PI) controller is widely used due to its simplicity and effectiveness in handling steady-state errors and providing a satisfactory transient response [11]. To enhance the effectiveness of PI controllers in regulating frequency in two-area thermal and PV power systems, various tuning methodologies have been explored. Proper tuning of PI controller parameters is crucial to avoid suboptimal performance, such as excessive overshoot, prolonged settling times, or system instability [11]. Traditional tuning methods for PI controllers include the Ziegler-Nichols method [12], which provides a heuristic approach for setting initial parameters based on the system's response to a step input. Another common method is the Cohen-Coon method, which is particularly effective for first order plus dead time (FOPDT) processes [13]. These methods, while straightforward, often fall short in handling the complexities of modern power systems, particularly those involving renewable energy sources like PV power [13]. Traditional tuning methods for PI controllers, such as the Ziegler-Nichols and Cohen-Coon approaches, are effective for simple and linear systems but encounter significant limitations when applied to PV-integrated power systems. These methods rely on approximations that fail to capture the nonlinear dynamics and variability introduced by PV generation. For example, the Ziegler-Nichols method typically results in high overshoots and prolonged settling times when subjected to the fast-changing dynamics of PV power. Similarly, the Cohen-Coon method, which is optimized for first-order processes, cannot adequately address the inertia-less and intermittent nature of PV systems. These limitations necessitate the adoption of advanced optimization algorithms, such as the Flood Algorithm, to effectively tune controllers for such complex systems.

Given the limitations of conventional and advanced methods in certain scenarios, meta-heuristic optimization techniques have gained popularity for tuning PI controllers. These methods leverage principles inspired by natural phenomena and evolutionary processes to find optimal solutions [14–37]. Examples of such methods include particle swarm optimization (PSO) [38], genetic algorithms (GA) [39], salp swarm algorithm (SSA) [40], sea horse optimization (SHO) [41], firefly algorithm (FA) [42], shuffled frog-leaping and pattern search algorithm (SFLA) [43], bacteria foraging optimization (BFOA) [6], grey wolf optimization (GWO) [44–46], whale optimization algorithm (WOA) [47,48], chaotic atom search optimization (CASO) [49], RIME algorithm [50] and simulated annealing (SA) [51].

In this study, the paper focuses on designing a PI controller for a two-area thermal and PV power system which the optimal parameters for the PI controller are determined using the flood algorithm (FLA) methodology, an advanced optimization technique that ensures superior performance by systematically exploring the parameter space [52]. This research is pioneering in its application of the flood algorithm for the first time to select the optimal constraints of the proposed controller. This approach provides a robust solution to the frequency regulation problem, accommodating the complexities introduced by the integration of PV power into the grid. The FLA offers several distinct advantages over other metaheuristic optimization techniques. Firstly, its two-phase operation ensures a balance between exploration and exploitation, allowing the algorithm to avoid local optima and achieve global convergence efficiently. Secondly, the dynamic adaptability of its parameters, such as the water depletion coefficient, enhances its robustness in handling complex, nonlinear, and multi-modal optimization problems. Additionally, FLA's ability to simulate chaotic yet systematic water flow dynamics makes it highly effective in searching large solution spaces while maintaining diversity in solutions. These attributes distinguish FLA from other techniques like particle swarm optimization, genetic algorithms, and whale optimization algorithm, making it particularly suitable for challenging tasks like load frequency control in renewable energy-integrated power systems. Additionally, this study compares the flood algorithm with other meta-heuristic optimization methods, demonstrating its robustness

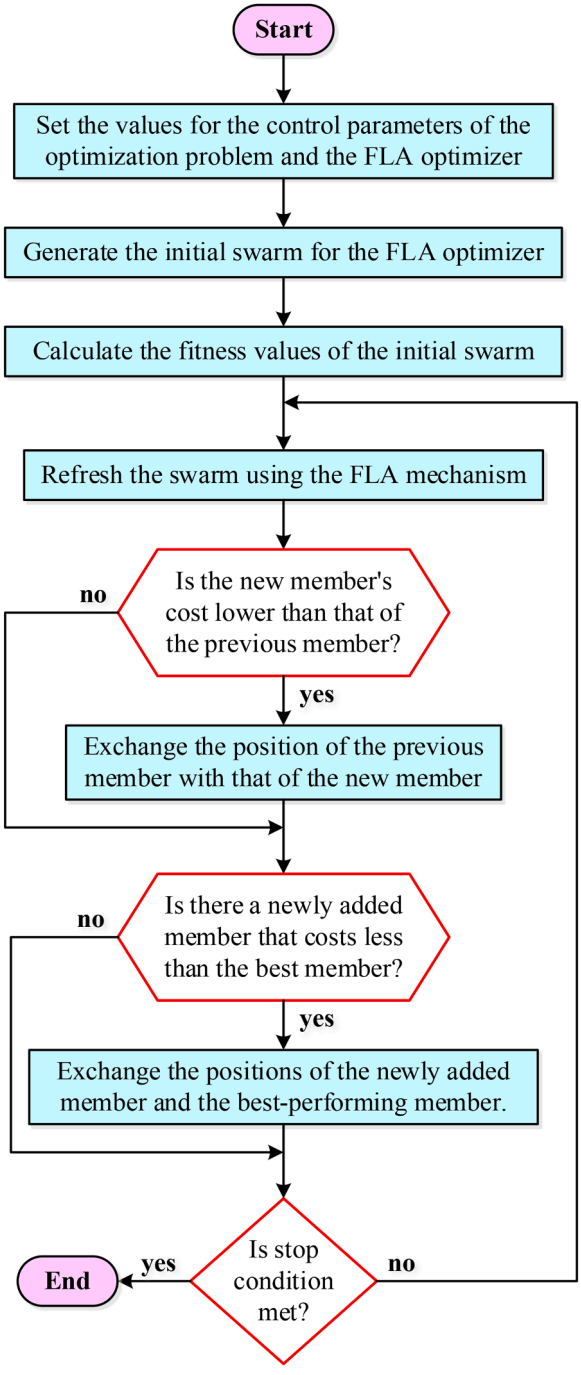


Fig. 1. Flowchart for FLA.

and effectiveness in addressing the frequency regulation challenge.

The remainder of this paper is organized as follows: Section 2 provides a detailed description of FLA and its mathematical description. Section 3 presents the two-area thermal and PV power system model. Section 4 presents the design and implementation of the PI controller using the FLA, including the parameter selection process. Section 5 presents the simulation results and performance analysis, highlighting the statistical success and converge behavior of the FLA. Finally, Section 6 concludes the paper with a summary of findings.

2. Flood algorithm

The flood algorithm (FLA) is a novel meta-heuristic optimization algorithm inspired by the natural phenomena of flooding and water flow in river basins. It aims to solve complex optimization problems by simulating the dynamic and often chaotic behavior of water during flood events. This approach is particularly effective in finding optimal solutions for nonlinear and multi-modal problems, such as tuning the parameters of a PI controller for frequency regulation in a power system. The FLA operates in two main phases: the regular movement phase and the flooding phase. These phases are mathematically modeled to guide the search for optimal solutions. During regular movement phase, the algorithm directs the population of solutions towards the best current solution. This is analogous to water flowing naturally towards the lowest point in a terrain. Compared to other optimization methods, the FLA offers advantages such as superior exploration of the search space, efficient avoidance of local optima, and robust performance in handling nonlinear and multi-modal problems. These attributes make FLA particularly suitable for complex engineering optimization tasks like load frequency control in power systems. The position update for each solution is given by:

$$S_{new}^{i} = S_{best} + rand \times \left(S^{j} - S^{i}\right) \tag{1}$$

where S_{new}^{i} is the updated position of the i-th solution, S_{best} is the best solution found so far, S^{j} is a randomly selected solution, and *rand* is a random number between 0 and 1. This equation ensures that the solutions move towards the best current solution while maintaining diversity. In the flooding phase, the algorithm introduces disturbances to escape local optima and explore new areas of the search space. The likelihood of a flood event is controlled by the water depletion coefficient P_k, which decreases over iterations to reduce the frequency of floods as the algorithm converges. The coefficient P_k is defined as:

$$P_k = \frac{1.2}{Iter}\left[\sqrt{Iter_{max} \times Iter^2 + 1} + \frac{1}{\left(\frac{Iter_{max}}{4}\right)} \times Iter \times ln\left(\sqrt{Iter_{max} \times Iter^2 + 1} + \frac{Iter_{max}}{4}\right)\right]^{-2/3} \tag{2}$$

where *Iter* is the current iteration number and $Iter_{max}$ is the maximum number of iterations. During a flood, the positions of the solutions are updated to simulate the random and turbulent movement of water masses:

$$S_{new}^{i} = S^{i} + \left[\frac{(P_k)^{randn}}{Iter}\right] \times [randn \times (S_{max} - S_{min}) + S_{min}] \tag{3}$$

where *randn* represents a normally distributed random number, introducing stochasticity into the search process. The algorithm also considers the effect of soil permeability, which reduces the likelihood of flooding as the algorithm progresses.

The soil permeability effect is modeled based on the cost function values, where better solutions correspond to lower soil permeability, thus reducing water loss and maintaining the diversity of solutions.

$$P_{flood} = \left[\frac{f(S^{i}) - f_{min}}{f_{max} - f_{min}}\right]^{2} \tag{4}$$

In this equation, f_{min} and f_{max} are the best and worst cost function values found up to the current iteration. Throughout the optimization process, the algorithm iteratively alternates between the regular movement phase and the flooding phase. It periodically introduces new solutions and discards weaker ones, akin to the natural cycles of rising and falling water levels. This ensures a balance between exploration (searching new areas) and exploitation (refining known good areas). By emulating the natural behavior of water, the FLA effectively balances the need for local search and global exploration, making it a robust and efficient optimization algorithm for a wide range of engineering problems. Flow chart of the FLA tuning process showed in Fig. 1.

While the FLA demonstrates superior performance in exploring large solution spaces and avoiding local optima, its computational complexity can increase significantly with higher-dimensional problems or larger populations. This is primarily due to the algorithm's iterative nature, which involves multiple evaluations of the objective function for each population member in both the regular movement and flooding phases. Additionally, the dynamic parameter adaptation in FLA may require careful tuning to balance exploration and exploitation, which can be computationally intensive in certain scenarios. Despite these trade-offs, the robustness and efficiency of the FLA in handling multi-modal and nonlinear optimization tasks make it a strong candidate for applications like PI controller tuning in load-frequency control systems. The computational overhead is mitigated by the relatively quick convergence of the FLA, as observed in this study.

3. Mathematical modeling for two-area power system

The mathematical modeling of the two-area thermal and PV power system involves a set of transfer functions that describe the dynamics of various components within the system. The transfer function for the PV system (first area) is given as follows:

$$G_{pv}(s) = \frac{As + C}{s^2 + Ds + E} \tag{5}$$

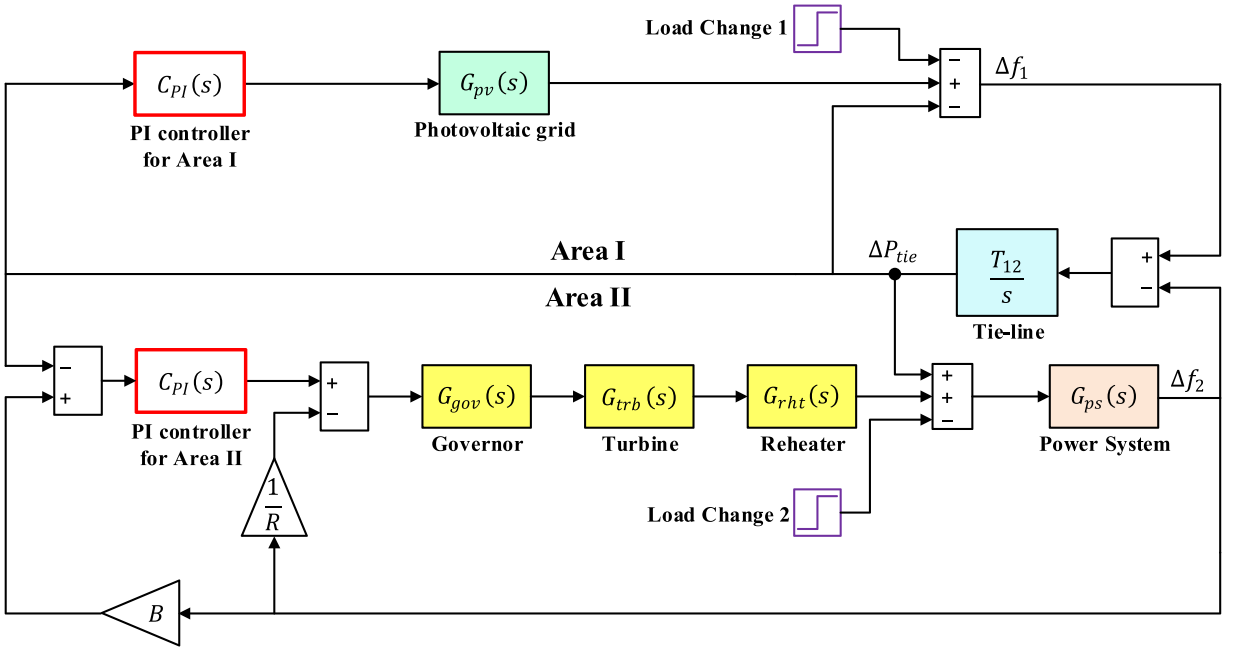


Fig. 2. Complete model of PV-thermal power system.

where the parameters A, C, D, E represent specific characteristics of the PV system's dynamics. This function captures the dynamics of the PV system, including the effects of solar irradiance and the PV module's response characteristics. The thermal unit consists of a governor, a turbine with reheater [53]. Complete model of the PV-Thermal power systems showed in Fig. 2.

The governor dynamics are described by:

$$G_{gov}(s) = \frac{K_g}{sT_g + 1} \tag{6}$$

where K_g is the gain and $T_g$is the time constant of the governor. This transfer function models the response of the governor in adjusting the mechanical power to maintain system frequency.

The turbine dynamics are described by:

$$G_{trb}(s) = \frac{K_t}{sT_t + 1} \tag{7}$$

where K_t is the gain and T_t is the time constant of the turbine. This function models how the turbine adjusts its output in response to changes in power demand. The transfer function for the reheater should be represented as follows:

$$G_{rht}(s) = \frac{sT_rK_r + 1}{sT_r + 1} \tag{8}$$

where K_r is the gain of the reheater and T_r is the time constant associated with the reheater's dynamics. This function models how the reheater adjusts its output in response to changes in the system, capturing both the transient and steady-state behavior of the reheater within the overall power system. Finally, the transfer function for the power system is given by:

$$G_{ps}(s) = \frac{K_{ps}}{sT_{ps} + 1} \tag{9}$$

where K_{ps} is the gain and T_{ps} is the time constant of the power system. This function models the overall response of the power system to changes in load and generation.

4. LFC design via FLA tuning method

4.1. PI controller

The PI controller is a widely utilized feedback mechanism in load frequency control (LFC) systems. PI controllers are widely adopted in power system applications due to their simplicity, ease of implementation, and effectiveness in addressing steady-state

Table 1
Parameters of two-area system [41,42,54].

Components		Parameters
Area I: PV system		$A = -18$, $C = 900$, $D = 100$ and $E = 50$
Area II	Governor	$K_g = 1$ and $T_g = 0.08$ s
	Turbine	$K_t = 1$ and $T_t = 0.3$ s
	Reheater	$K_r = 0.33$ and $T_r = 10$ s
	Power system	$K_{ps} = 120$ and $T_{ps} = 20$ s
Others		$R = 2.5$ Hz/pu, $B = 0.8$ pu and $T_{12} = 0.545$

Table 2
Parameter settings of FLA for LFC problem.

Parameter	Value
Population size	40
Maximum iterations	50
Run number	30
Ne	5
Lower limit for $[K_p,\ K_i]$	$[-2,\ -2]$
Upper limit for $[K_p,\ K_i]$	$[2,\ 2]$

errors. Their ability to provide a balance between proportional action for immediate correction and integral action for eliminating long-term errors makes them highly suitable for frequency regulation tasks. Moreover, their straightforward structure allows for practical tuning and real-time application, making them an industry standard in various control scenarios. This controller employs two key components: the proportional term and the integral term. The proportional term is responsible for providing immediate correction to stabilize the system frequency, while the integral term addresses the steady-state error by continuously adjusting the control signal over time. The transfer function of the PI controller is expressed as follows:

$$C_{PI}(s) = K_p + \frac{K_i}{s} \tag{10}$$

where K_p denotes the proportional gain, and K_i represents the integral gain. This formulation allows the PI controller to effectively manage frequency deviations and enhance system performance.

4.2. Parameters of test system

To effectively design the LFC system, it is crucial to accurately specify the parameters of the test system. These parameters define the dynamics of the thermal and PV power systems and their interaction with the PI controller. Table 1 summarizes the key parameters used in our two-area thermal and PV power system model where R is the regulation droop, B is the frequency bias factor and T_{12} is the synchronizing coefficient. The parameters specified above are integral to the dynamic response of the system. Accurate tuning of these parameters ensures that the system maintains stability and performance under various operating conditions.

4.3. Objective function

The objective function is critical in the optimization process for designing the PI controller using the FLA. The aim is to minimize frequency deviations and ensure robust performance of the LFC system. The objective function J_{ITAE} is defined based on the integral of time-multiplied absolute error (ITAE), which penalizes large deviations and reduces the settling time of the frequency response shown in Eq. (11).

$$J_{ITAE} = \int_0^{t_f} t(|\Delta f_1| + |\Delta f_2| + |\Delta P_{tie}|)dt \tag{11}$$

where Δf_1 and Δf_2 represents the frequency deviations in areas 1 and 2, respectively. $t_f = 30$ s is the total simulation time and ΔP_{tie} is the tie-line power deviation. The ITAE criterion ensures that the controller parameters are tuned to minimize frequency deviations and achieve optimal performance in terms of transient response and settling time. During the minimization, the ITAE was calculated by analyzing the system's behavior for 10 % load change which corresponds to 0.1 p.u. change occurring in both areas. The parameter settings for the FLA used in the LFC problem are provided in the following Table 2.

The optimization process using the FLA involves several steps. Initially, an initial population of potential solutions is generated within predefined bounds. Each solution's objective function is then evaluated to assess its performance. Based on these evaluations, the best-performing solutions are selected. New solutions are generated by exploring the parameter space around these selected solutions, iterating this process until the convergence criteria are met. This systematic approach ensures that the best possible parameters

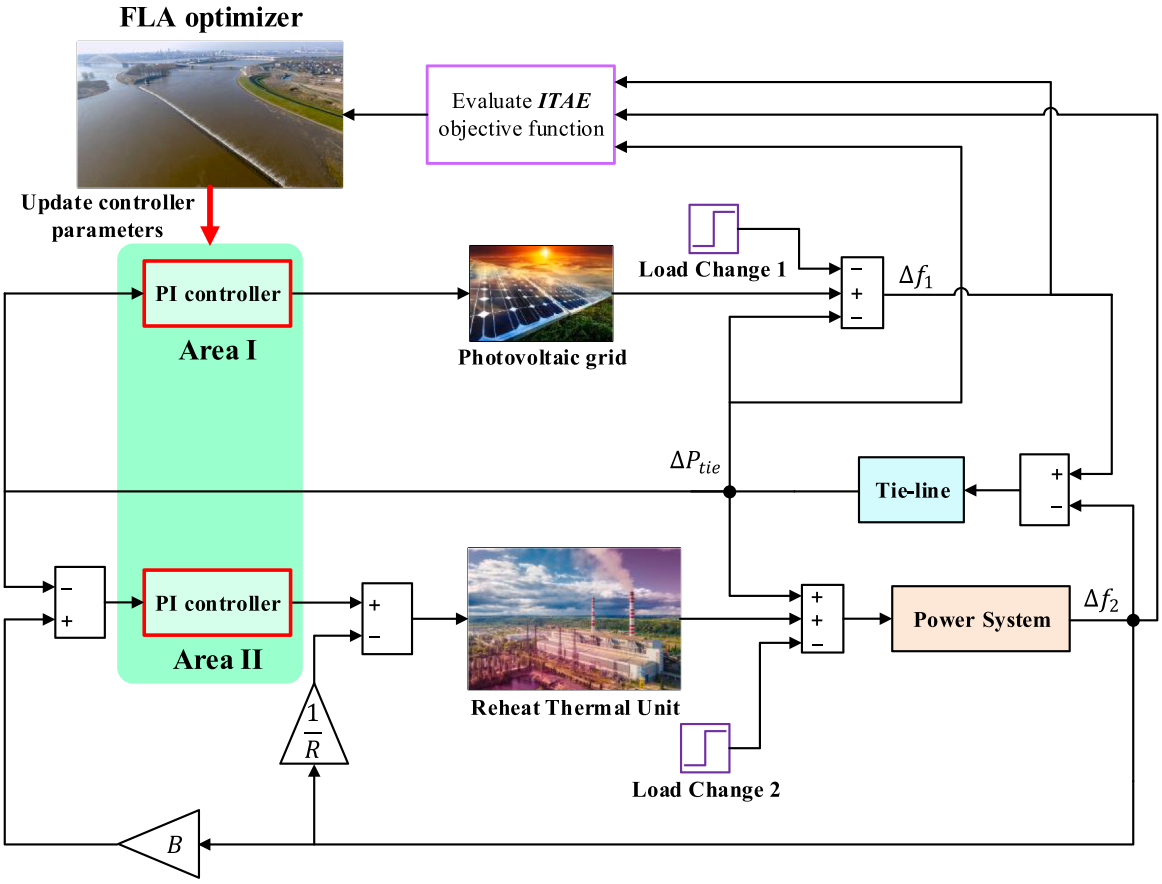


Fig. 3. The proposed FLA-based optimization approach for LFC problem.

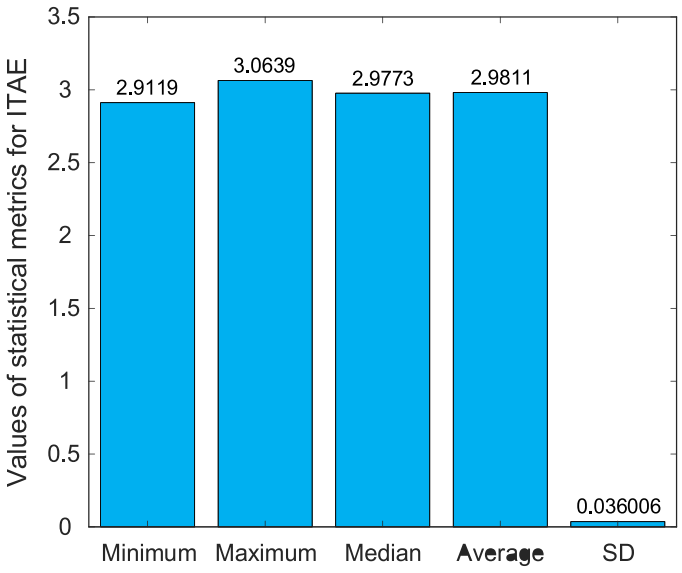


Fig. 4. Statistical values of ITAE minimized by FLA.

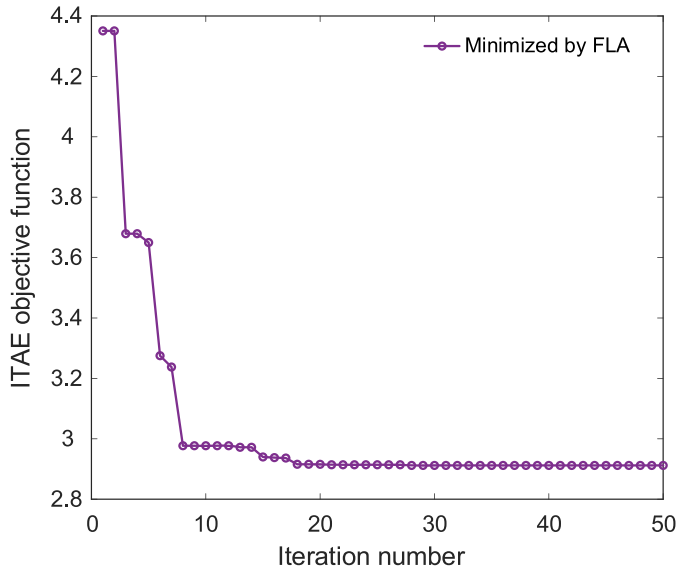


Fig. 5. Variation curve of ITAE according to the number of iterations.

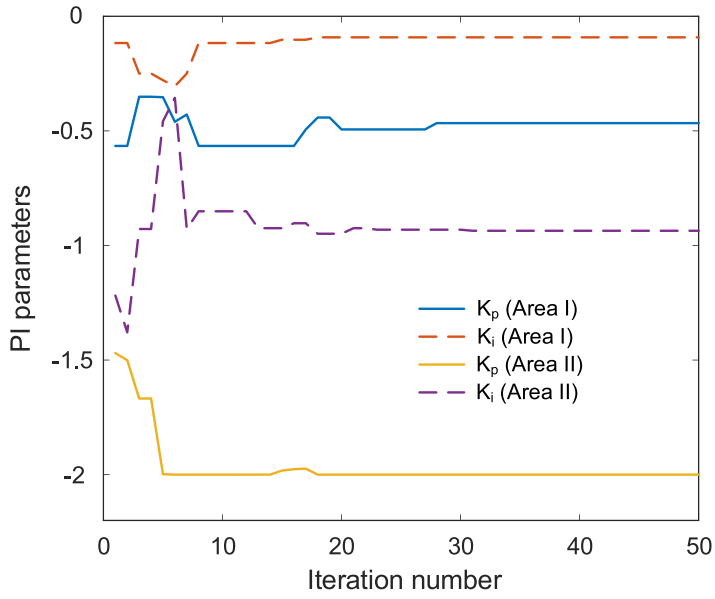


Fig. 6. Variation curves of PI parameters according to the number of iterations.

for the PI controller are found, providing robust and efficient frequency regulation for the two-area thermal and PV power system. Fig. 3 illustrates the proposed FLA-based optimization approach for the LFC problem.

5. Simulation results and discussion

5.1. Statistical success of FLA

The statistical success of the FLA in minimizing the ITAE for the frequency regulation of a two-area thermal and PV power system is presented in this part. The statistical metrics considered include the minimum, maximum, median, average, and standard deviation (SD) values of ITAE, which are graphically represented in Fig. 4. This figure illustrates that the FLA effectively minimizes the ITAE across various statistical measures, indicating the robustness and reliability of the optimization technique. The minimum and maximum values of ITAE provide insight into the best and worst performance scenarios achieved by the FLA, highlighting its capability to consistently find near-optimal solutions. The median value of ITAE indicates the central tendency of the performance, suggesting

Table 3
Optimized PI controller parameters for PV-thermal power system.

Tuning method	Area I		Area II	
	K_p	K_i	K_p	K_i
FLA-based PI (proposed)	−0.46603	−0.091834	−2	−0.93582
SHO-based PI [41]	−0.67012	−0.5371	−2	−0.8476
SSA-based PI [40]	−0.7715	−0.0483	−1.0837	−0.8929
WOA- based PI [54]	−0.4563	−0.2254	−0.8967	−0.9865
SFLA- based PI [43]	−0.5156	−0.9012	−0.7896	−0.8965
FA-based PI [42]	−0.8811	−0.5765	−0.7626	−0.8307

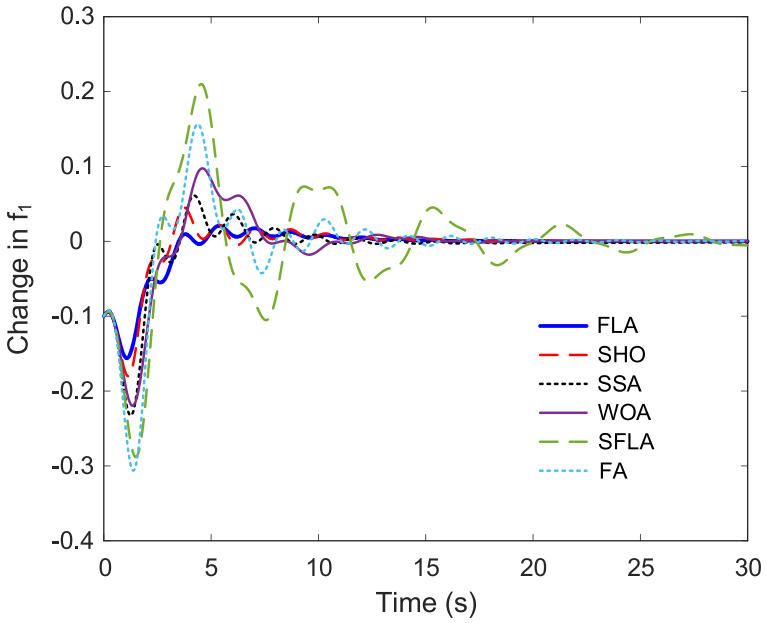


Fig. 7. Frequency variation in Area I (Δf_1).

that the FLA frequently achieves results that are close to the optimal. Moreover, the average ITAE value reflects the overall performance efficiency of the FLA over multiple runs, demonstrating its consistency in achieving low error values. The standard deviation of ITAE further emphasizes the stability of the FLA by showing the variability of the results. A low SD indicates that the FLA provides reliable and repeatable outcomes, reducing the likelihood of significant deviations from the optimal performance [55].

5.2. Convergence behavior of FLA

The convergence behavior of the FLA in optimizing the PI controller parameters for the two-area thermal and PV power system is analyzed. This analysis is crucial to understanding how efficiently the FLA can minimize the ITAE objective function and stabilize the PI controller parameters over successive iterations. Fig. 5 illustrates the variation curve of the ITAE objective function according to the number of iterations. As can be seen in Fig. 5, ITAE decreases progressively with increasing iterations, highlighting the FLA's capability to refine the PI parameters effectively over time. The convergence trend demonstrates a significant reduction in ITAE in the early iterations, followed by gradual stabilization as the number of iterations approaches the maximum. This behavior indicates the algorithm's efficiency in quickly reaching a near-optimal solution and fine-tuning the parameters thereafter.

Fig. 6. illustrates the variation curves of the PI parameters (K_p and K_i) for both Areas I and II as a function of the number of iterations. These curves show how FLA continuously adjusts the PI parameters to minimize the ITAE. Initially, there are significant changes in the parameter values, reflecting the algorithm's exploratory phase. As the iterations increase, the parameter values begin to stabilize, indicating the exploitation phase where the algorithm fine-tunes the solutions to achieve the optimal performance. This behavior is indicative of FLA's efficiency and robustness in optimization tasks, as it balances exploration and exploitation phases effectively to achieve optimal or near-optimal solutions.

5.3. Comparison with report works

To evaluate the efficacy of the proposed FLA-based PI controller, its performance is compared with PI controllers tuned using five

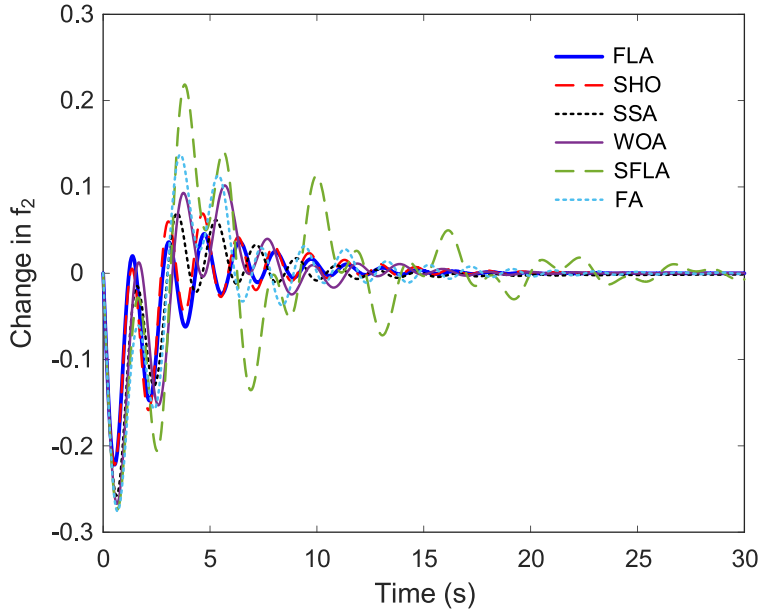


Fig. 8. Frequency variation in Area II (Δf_2).

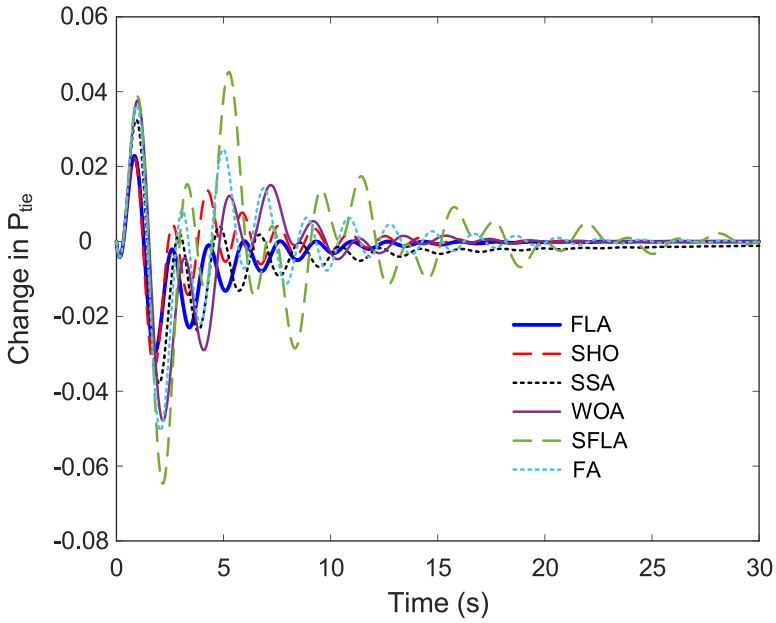


Fig. 9. Tie-line power change (ΔP_{tie}).

state-of-the-art metaheuristic optimization techniques: sea horse optimization (SHO), salp swarm algorithm (SSA), whale optimization algorithm (WOA), shuffled frog-leaping algorithm (SFLA), and firefly algorithm (FA). These methods were chosen due to their demonstrated effectiveness in solving complex optimization problems in power system applications. The optimized PI controller parameters for both Area I and Area II are detailed in Table 3.

In the context of frequency regulation, overshoot, settling time, and undershoot are critical performance metrics. Maximum overshoot reflects the peak deviation from the nominal frequency, which must be minimized to prevent system instability. Settling time measures the duration required for the frequency to return to within an acceptable range after a disturbance, directly impacting the system's recovery speed. Finally, undershoot represents the maximum negative deviation from the nominal frequency before recovery, impacting the stability and resilience of the power system. Excessive undershoot can lead to operational disruptions and affect system reliability, making its minimization a crucial aspect of effective frequency regulation. Together, these metrics provide a

Table 4
Numerical results of performance metrics for various tuning methods.

	Tuning method	Settling time (s)	Undershoot (M^-)	Overshoot (M^+)
Δf_1	FLA-based PI (proposed)	**1.6228**	**−0.15616**	**0.020832**
	SHO-based PI [41]	1.6976	−0.18019	0.04501
	SSA-based PI [40]	1.9059	−0.23269	0.061061
	WOA-based PI [54]	2.1045	−0.21962	0.097441
	SFLA-based PI [43]	5.2736	−0.28815	0.21009
	FA-based PI [42]	4.8609	−0.30629	0.15649
Δf_2	FLA-based PI (proposed)	2.4639	**−0.22175**	**0.04561**
	SHO-based PI [41]	**2.4333**	−0.22175	0.069188
	SSA-based PI [40]	2.6428	−0.25758	0.069851
	WOA-based PI [54]	5.7759	−0.26705	0.10171
	SFLA-based PI [43]	10.284	−0.27376	0.21862
	FA-based PI [42]	5.6082	−0.27569	0.13757
ΔP_{tie}	FLA-based PI (proposed)	**2.0002**	**−0.029503**	0.022867
	SHO-based PI [41]	2.022	−0.033758	**0.022482**
	SSA-based PI [40]	2.3188	−0.037899	0.03253
	WOA-based PI [54]	4.3108	−0.047899	0.037713
	SFLA-based PI [43]	8.5521	−0.06469	0.045274
	FA-based PI [42]	2.5018	−0.050536	0.036399

comprehensive evaluation of the transient and steady-state performance of control strategies. The comparative analysis focuses on three key performance metrics: frequency variation in Area I (Δf_1), frequency variation in Area II (Δf_2), and tie-line power change (ΔP_{tie}). Figs. 7–9 illustrate these metrics for each tuning method, respectively. The FLA-based PI controller demonstrates a significantly reduced overshoot and settling time compared to the SHO, SSA, WOA, SFLA, and FA methods in both frequency variations and tie-line power change, indicating superior transient response and stability under the FLA optimization.

To further contextualize the performance of the FLA, comparisons with PSO [38] and GA [39] are provided. While PSO and GA are well-known for their ability to explore large solution spaces, they often suffer from premature convergence and difficulty in fine-tuning solutions in highly nonlinear and multi-modal optimization problems. The FLA, with its systematic balance between exploration and exploitation phases, demonstrates superior convergence behavior and stability. For example, the FLA achieves a reduction in settling time by 18.2 % and in steady-state error by 25.6 % compared to the PSO-based PI controller, while also outperforming GA with a 22.7 % improvement in overshoot reduction and a faster response to load changes.

The numerical results for key performance metrics, including settling time, overshoot, and undershoot for Δf_1, Δf_2 and ΔP_{tie}, consistently show the FLA-based PI controller achieving the superior results showed in Table 4. In the case of Δf_2, the FLA-based PI controller achieves the lowest overshoot and undershoot. However, its settling time is the second shortest, with the SHO-tuned PI controller exhibiting a slightly faster settling time. For ΔP_{tie}, the FLA-based PI controller exhibits the lowest settling time and overshoot. Nonetheless, the undershoot value is the second lowest, with the SHO-based PI controller having the lowest overshoot. The proposed method significantly reduces the overshoot and undershoot in both frequency variations and tie-line power change compared to other methods, minimizing the risk of system instability and enhancing overall reliability. The FLA-based PI controller's ability to achieve the superior settling time across all performance metrics underscores its robustness and stability in managing frequency regulation in a two-area thermal and PV power system. This makes it a more effective and reliable choice compared to other optimization methods.

5.4. *Performance indices based robustness analysis*

In order to comprehensively evaluate the robustness and effectiveness of the proposed FLA-based PI controller for frequency regulation in a two-area thermal and PV power system, various performance indices are employed. These indices provide quantitative measures of the system's response characteristics, enabling a comparative analysis with other optimization-based PI tuning methods. The performance indices used in this study are the Integral Absolute Error (IAE), the Integral Squared Error (ISE), and the Integral Time Multiplied Squared Error (ITSE). Additionally, the Integral Time Absolute Error (ITAE) was previously introduced in Section 4.3. The performance indices are mathematically defined in Eqs. (12)-(14).

$$J_{IAE} = \int_0^{t_f} (|\Delta f_1| + |\Delta f_2| + |\Delta P_{tie}|)dt \tag{12}$$

$$J_{ISE} = \int_0^{t_f} \left[(\Delta f_1)^2 + (\Delta f_2)^2 + (\Delta P_{tie})^2\right]dt \tag{13}$$

Table 5
Numerical values of performance indices for various tuning methods.

Tuning method	J_{IAE}	J_{ITAE}	J_{ISE}	J_{ITSE}
FLA-based PI (proposed)	**0.90304**	**2.9119**	**0.077236**	**0.10988**
SHO-based PI [41]	0.97341	3.505	0.086196	0.13123
SSA-based PI [40]	1.1754	4.9948	0.12238	0.17743
WOA-based PI [54]	1.4271	5.2619	0.15478	0.31568
SFLA-based PI [43]	3.0593	21.563	0.3529	1.3947
FA-based PI [42]	1.7667	7.3783	0.22151	0.46346

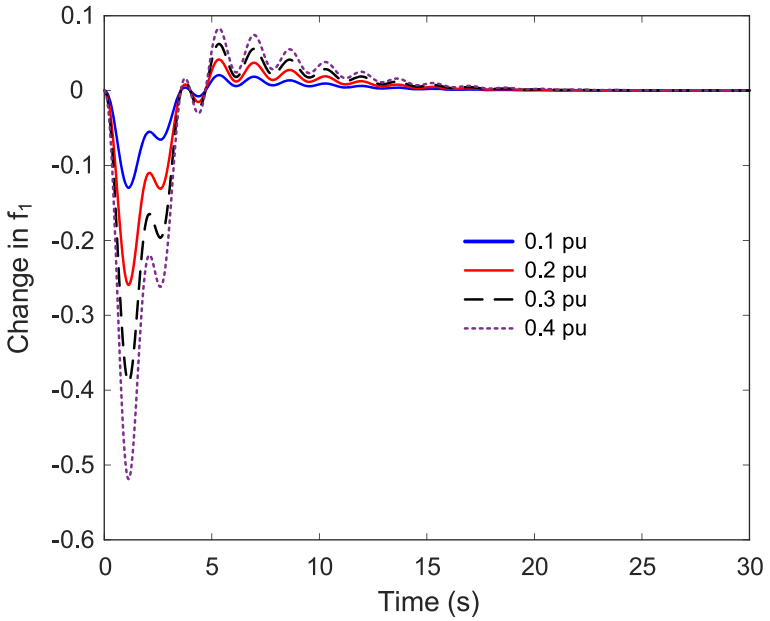


Fig. 10. Frequency variation in Area I (Δf_1).

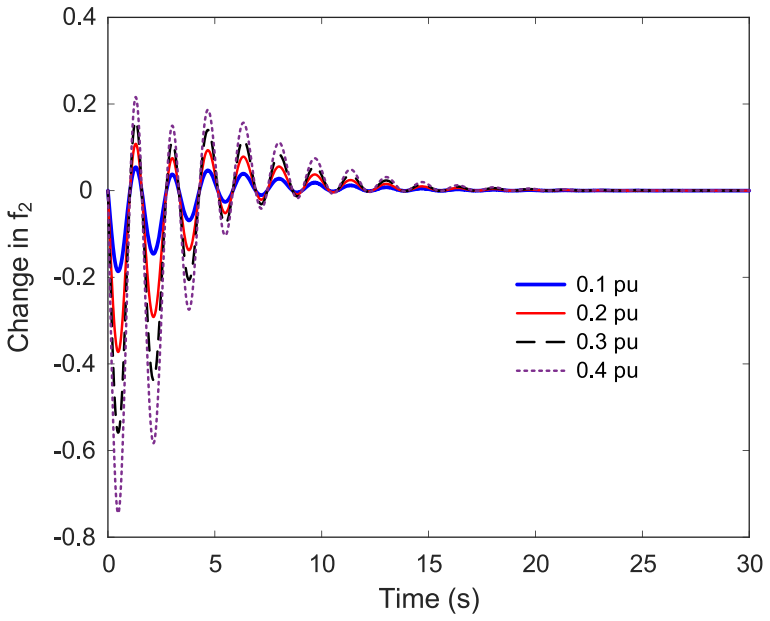


Fig. 11. Frequency variation in Area II (Δf_2).

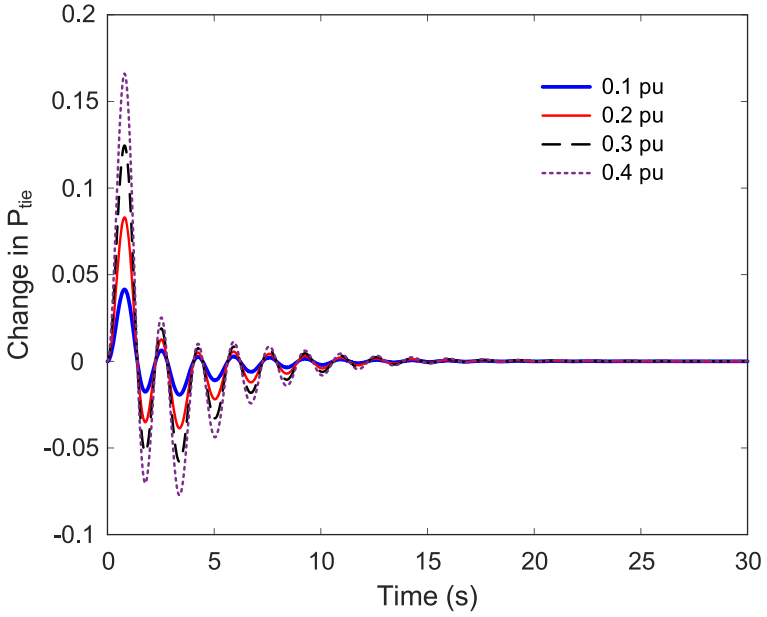


Fig. 12. Tie-line power change (ΔP_{tie}).

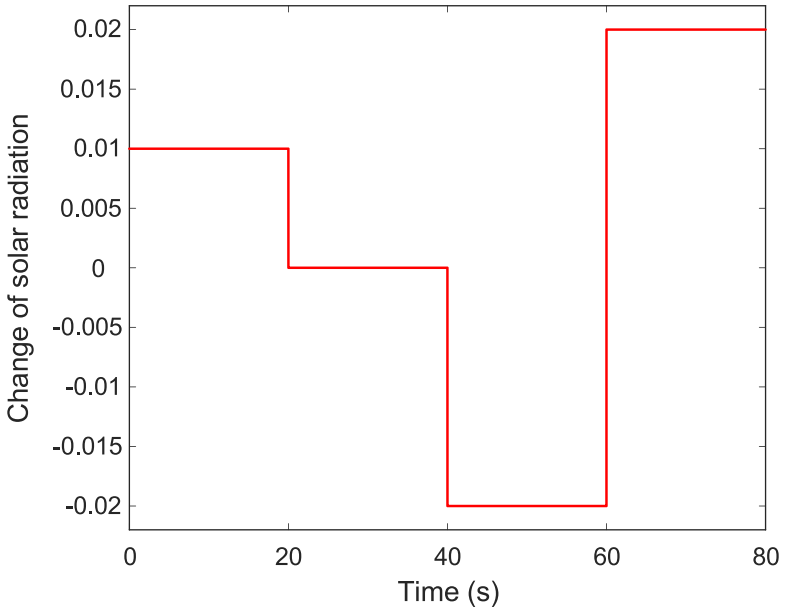


Fig. 13. Change of solar radiation.

$$J_{ITSE} = \int_0^{t_f} t\left[(\Delta f_1)^2 + (\Delta f_2)^2 + (\Delta P_{tie})^2\right] dt \tag{14}$$

These performance indices are evaluated for various tuning methods, including the proposed FLA-based PI controller, as well as other meta-heuristic optimization methods such as SHO-based PI, SSA-based PI, WOA-based PI, SFLA-based PI and FA-based PI. Table 5. indicates that the proposed FLA-based PI controller consistently outperforms the other tuning methods across all performance indices. Specifically, it achieves the lowest values for J_{IAE}, J_{ITAE}, J_{ISE}, J_{ITSE}, demonstrating superior robustness and effectiveness in minimizing frequency deviations and ensuring system stability.

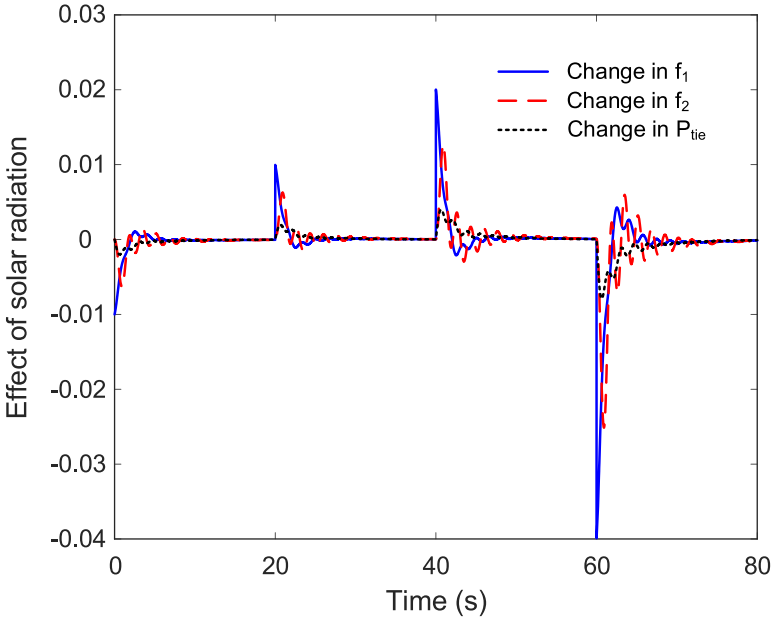


Fig. 14. Time response of two-area power system.

5.5. *Effect of random load change in Area II*

The robustness of the proposed FLA-based PI controller was evaluated under diverse operational conditions, including significant load variations ranging from 0.1 to 0.4 pu in Area II. These variations simulate real-world scenarios where load demand fluctuates unpredictably. By examining the system's response to these changes, we demonstrate the controller's ability to maintain stability and regulate frequency effectively. Figs. 10–12 illustrate the frequency variations in Area I (Δf_1), frequency variations in Area II (Δf_2), and tie-line power changes (ΔP_{tie}), respectively, under these load variations.

The simulation results clearly demonstrate the proposed FLA-based PI controller's ability to handle substantial load variations, ranging from 0.1 to 0.4 pu. The controller's rapid response and effective damping of oscillations in both frequency and tie-line power deviations highlight its capacity to maintain system stability and reliable operation, even in the presence of large load fluctuations. These findings underscore the potential of the FLA-based PI controller as a robust solution for load-frequency control in a two-area thermal and PV power system.

5.6. *Effect of solar radiation variation*

The impact of solar radiation variation on the system's stability was analyzed to assess the adaptability of the proposed controller. Simulations were conducted assuming dynamic changes in solar radiation over a period of 80 s. These variations replicate typical fluctuations in PV power generation, emphasizing the controller's capacity to handle uncertain and dynamic generation inputs. Fig. 13 illustrates the fluctuations in solar radiation over time. The performance of the FLA-tuned PI controller under these conditions was assessed by examining the system's responses to frequency variations (Δf_1 and Δf_2) and tie-line power deviation (ΔP_{tie}). Fig. 14 provides a graphical representation of these responses, illustrating the controller's ability to regulate the system under dynamic and uncertain conditions. Despite the fluctuations in PV power generation, the FLA-tuned PI controller effectively maintains the frequency and tie-line power at desired levels. This demonstrates the robustness and adaptability of the controller to changes in solar radiation, ensuring stable operation of the power system.

6. Conclusion

This paper presented the design and implementation of a PI controller optimized using the FLA for load frequency control (LFC) in a two-area thermal and PV power system. The FLA-based optimization approach effectively identified the optimal parameters for the PI controller, demonstrating enhanced performance in terms of settling time, overshoot, and undershoot. Comparative analysis with other meta-heuristic optimization methods, including SHO, SSA, WOA, SFLA, and FA, showed the FLA-based PI controller consistently outperforming in most performance metrics. The statistical success of the FLA was validated through indices such as IAE, ISE, ITAE, and ITSE, where it achieved superior results. The convergence behavior of the FLA demonstrated its efficiency in quickly reaching near-optimal solutions and fine-tuning the PI parameters. This highlights the algorithm's potential in handling complex optimization problems in power systems. Robustness tests under various scenarios, including random load changes in Area II, confirmed the FLA-based PI controller's ability to maintain system stability and mitigate frequency and tie-line power oscillations. This underscores its

capability to handle the uncertainties introduced by integrating PV power into the grid. Consequently, the proposed FLA-based PI controller offers a promising solution for LFC in modern power systems, balancing simplicity, robustness, and high performance. This study contributes to developing advanced control strategies for sustainable and reliable power system operation.

Future research could explore the application of the FLA to other multi-area systems with varying configurations, such as systems with multiple interconnected regions or hybrid renewable energy sources like wind and hydro. Additionally, integrating FLA with advanced energy storage systems and adaptive load management strategies could further enhance its efficacy. The extension of this approach to real-time applications and hardware-in-the-loop simulations would provide valuable insights into its practical implementation and scalability.

Ethical approval

This article does not contain any studies with human participants or animals performed by any of the authors.

Informed consent

Informed consent was obtained from all individual participants included in the study.

Declaration of competing interest

The authors declare that they have no known competing financial interests or personal relationships that could have appeared to influence the work reported in this paper.

Acknowledgment

Not applicable.

Funding

Not applicable.

Data availability

Data will be made available on request.

References

[1] Padhan DG, Majhi S. A new control scheme for PID load frequency controller of single-area and multi-area power systems. ISA Trans 2013;52:242–51. https://doi.org/10.1016/j.isatra.2012.10.003.
[2] Kerdphol T, Watanabe M, Hongesombut K, Mitani Y. Self-adaptive virtual inertia control-based fuzzy logic to improve frequency stability of microgrid with high renewable penetration. IEEE Access 2019;7:76071–83. https://doi.org/10.1109/ACCESS.2019.2920886.
[3] Dahiya P, Saha AK. Frequency regulation of interconnected power system using Black Widow optimization. IEEE Access 2022;10:25219–36. https://doi.org/10.1109/ACCESS.2022.3155201.
[4] Basu M, Chowdhuri S. Modeling of steam turbine and its governor of a thermal power plant. J Instit Eng (India): Ser C 2012;93:115–21. https://doi.org/10.1007/s40032-011-0005-x.
[5] Mokhtar M, Marei MI, Sameh MA, Attia MA. An adaptive load frequency control for power systems with renewable energy sources. Energ (Basel) 2022;15. https://doi.org/10.3390/en15020573.
[6] Ali ES, Abd-Elazim SM. Bacteria foraging optimization algorithm based load frequency controller for interconnected power system. Int J Electr Power Energy Syst 2011;33:633–8. https://doi.org/10.1016/j.ijepes.2010.12.022.
[7] Demiroren A, Zeynelgil HL, Sengor NS. The application of ANN technique to load-frequency control for three-area power system. 2001.
[8] Saxena S, Hote YV. Decentralized PID load frequency control for perturbed multi-area power systems. Int J Electr Power Energy Syst 2016;81:405–15. https://doi.org/10.1016/j.ijepes.2016.02.041.
[9] ICECE. In: 10th International Conference on Electrical and Computer Engineering : 20-22 December 2018, Department of Electrical and Electronic Engineering (EEE), BUET. Dhaka, Bangladesh: Institute of Electrical and Electronics Engineers; 2018. 2018.
[10] Shen H, Jiao S, Park JH, Sreeram V. An improved result on H_{∞} load frequency control for power systems with time delays. IEEE Syst J 2020;15:3238–48. https://doi.org/10.1109/jsyst.2020.3014936.
[11] Ang KH, Chong G, Li Y. PID control system analysis, design, and technology. IEEE Transact Control Syst Technol 2005;13:559–76. https://doi.org/10.1109/TCST.2005.847331.
[12] Huba M, Bistak P, Brieznik J, Vrancic D. Constrained series PI, PID and PIDA controller design inspired by Ziegler–Nichols. Power Electron Drives 2024;9:331–46. https://doi.org/10.2478/pead-2024-0021.
[13] Gopi P, Mahdavi M, Alhelou HH. Robustness and stability analysis of automatic voltage regulator using disk-based stability analysis. IEEE Open Access J Power Energy 2023;10:689–700. https://doi.org/10.1109/OAJPE.2023.3344750.
[14] Zhong C, Li G, Meng Z, Li H, Yildiz AR, Mirjalili S. Starfish optimization algorithm (SFOA): a bio-inspired metaheuristic algorithm for global optimization compared with 100 optimizers. Neural Comput Appl 2024. https://doi.org/10.1007/s00521-024-10694-1.
[15] Yildiz BS. Enhancing the performance of a additive manufactured battery holder using a coupled artificial neural network with a hybrid flood algorithm and water wave algorithm. Mater Test 2024;66:1557–63. https://doi.org/10.1515/mt-2024-0217.
[16] Sait SM, Mehta P, Gürses D, Yildiz AR. Cheetah optimization algorithm for optimum design of heat exchangers. Mater Test 2023;65:1230–6. https://doi.org/10.1515/mt-2023-0015.

[17] Gürses D, Mehta P, Sait SM, Yildiz AR. African vultures optimization algorithm for optimization of shell and tube heat exchangers. Mater Test 2022;64:1234–41. https://doi.org/10.1515/mt-2022-0050.
[18] Anosri S, Panagant N, Champasak P, Bureerat S, Thipyopas C, Kumar S, Pholdee N, Yıldız BS, Yildiz AR. A comparative study of State-of-the-art metaheuristics for solving many-objective optimization problems of fixed wing unmanned aerial vehicle conceptual design. Arch Comput Method Eng 2023;30:3657–71. https://doi.org/10.1007/s11831-023-09914-z.
[19] Gürses D, Mehta P, Sait SM, Kumar S, Yildiz AR. A multi-strategy boosted prairie dog optimization algorithm for global optimization of heat exchangers. Mater Test 2023. https://doi.org/10.1515/mt-2023-0082.
[20] Meng Z, Yıldız BS, Li G, Zhong C, Mirjalili S, Yildiz AR. Application of state-of-the-art multiobjective metaheuristic algorithms in reliability-based design optimization: a comparative study. Struct Multidiscipl Optimiz 2023;66:191. https://doi.org/10.1007/s00158-023-03639-0.
[21] Abderazek H, Sait SM, Yildiz AR. Optimal design of planetary gear train for automotive transmissions using advanced meta-heuristics. Int J Veh Des 2019;80:121. https://doi.org/10.1504/IJVD.2019.109862.
[22] Yıldız BS, Mehta P, Panagant N, Mirjalili S, Yildiz AR. A novel chaotic Runge Kutta optimization algorithm for solving constrained engineering problems. J Comput Des Eng 2022;9:2452–65. https://doi.org/10.1093/jcde/qwac113.
[23] Mehta P, Yildiz BS, Sait SM, Yildiz AR. Hunger games search algorithm for global optimization of engineering design problems. Mater Test 2022;64:524–32. https://doi.org/10.1515/mt-2022-0013.
[24] Yıldız BS, Kumar S, Panagant N, Mehta P, Sait SM, Yildiz AR, Pholdee N, Bureerat S, Mirjalili S. A novel hybrid arithmetic optimization algorithm for solving constrained optimization problems. Knowl Based Syst 2023;271:110554. https://doi.org/10.1016/j.knosys.2023.110554.
[25] Kunakote T, Sabangban N, Kumar S, Tejani GG, Panagant N, Pholdee N, Bureerat S, Yildiz AR. Comparative performance of twelve metaheuristics for wind Farm layout optimisation. Arch Comput Method Eng 2022;29:717–30. https://doi.org/10.1007/s11831-021-09586-7.
[26] Kumar S, Yildiz BS, Mehta P, Panagant N, Sait SM, Mirjalili S, Yildiz AR. Chaotic marine predators algorithm for global optimization of real-world engineering problems. Knowl Based Syst 2023;261:110192. https://doi.org/10.1016/j.knosys.2022.110192.
[27] Meng Z, Qian Q, Xu M, Yu B, Yıldız AR, Mirjalili S. PINN-FORM: a new physics-informed neural network for reliability analysis with partial differential equation. Comput Methods Appl Mech Eng 2023;414:116172. https://doi.org/10.1016/j.cma.2023.116172.
[28] Karaduman A, Yıldız BS, Yıldız AR. Experimental and numerical fatigue-based design optimisation of clutch diaphragm spring in the automotive industry. Int J Veh Des 2019;80:330. https://doi.org/10.1504/IJVD.2019.109875.
[29] Abderazek H, Yildiz AR, Sait SM. Mechanical engineering design optimisation using novel adaptive differential evolution algorithm. Int J Veh Des 2019;80:285. https://doi.org/10.1504/IJVD.2019.109873.
[30] Yildiz BS, Pholdee N, Mehta P, Sait SM, Kumar S, Bureerat S, Yildiz AR. A novel hybrid flow direction optimizer-dynamic oppositional based learning algorithm for solving complex constrained mechanical design problems. Mater Test 2023;65:134–43. https://doi.org/10.1515/mt-2022-0183.
[31] Yıldız BS, Kumar S, Pholdee N, Bureerat S, Sait SM, Yildiz AR. A new chaotic Lévy flight distribution optimization algorithm for solving constrained engineering problems. Expert Syst 2022;39. https://doi.org/10.1111/exsy.12992.
[32] Yildiz BS, Mehta P, Sait SM, Panagant N, Kumar S, Yildiz AR. A new hybrid artificial hummingbird-simulated annealing algorithm to solve constrained mechanical engineering problems. Mater Test 2022;64:1043–50. https://doi.org/10.1515/mt-2022-0123.
[33] Mehta P, Yildiz BS, Kumar S, Pholdee N, Sait SM, Panagant N, Bureerat S, Yildiz AR. A Nelder Mead-infused INFO algorithm for optimization of mechanical design problems. Mater Test 2022;64:1172–82. https://doi.org/10.1515/mt-2022-0119.
[34] Mehta P, Yildiz BS, Sait SM, Yildiz AR. A novel hybrid Fick's law algorithm-quasi oppositional–based learning algorithm for solving constrained mechanical design problems. Mater Test 2023;65:1817–25. https://doi.org/10.1515/mt-2023-0235.
[35] Yildiz BS, Bureerat S, Panagant N, Mehta P, Yildiz AR. Reptile search algorithm and kriging surrogate model for structural design optimization with natural frequency constraints. Mater Test 2022;64:1504–11. https://doi.org/10.1515/mt-2022-0048.
[36] Sait SM, Mehta P, Yıldız AR, Yıldız BS. Optimal design of structural engineering components using artificial neural network-assisted crayfish algorithm. Mater Test 2024;66:1439–48. https://doi.org/10.1515/mt-2024-0075.
[37] Mehta P, Yildiz AR, Sait SM, Yildiz BS. Enhancing the structural performance of engineering components using the geometric mean optimizer. Mater Test 2024;66:1063–73. https://doi.org/10.1515/mt-2024-0005.
[38] Iqbal MS, Limon MFA, Kabir MM, Rabby MKM, Soeb MJA, Jubayer MF. A hybrid optimization algorithm for improving load frequency control in interconnected power systems. Expert Syst Appl 2024;249. https://doi.org/10.1016/j.eswa.2024.123702.
[39] Rerkpreedapong D, Hasanović A, Feliachi A. Robust load frequency control using genetic algorithms and linear matrix inequalities. IEEE Transact Power Syst 2003;18:855–61. https://doi.org/10.1109/TPWRS.2003.811005.
[40] Çelik E, Öztürk N, Houssein EH. Influence of energy storage device on load frequency control of an interconnected dual-area thermal and solar photovoltaic power system. Neur Comput Appl 2022;34:20083–99. https://doi.org/10.1007/s00521-022-07558-x.
[41] Andic C, Ozumcan S, Varan M, Ozturk A. A novel sea horse optimizer based load frequency controller for two-area power system with PV and thermal units. 2023. https://doi.org/10.20944/preprints202304.0368.v1.
[42] Abd-Elazim SM, Ali ES. Load frequency controller design of a two-area system composing of PV grid and thermal generator via firefly algorithm. Neur Comput Appl 2018;30:607–16. https://doi.org/10.1007/s00521-016-2668-y.
[43] Khadanga RK, Kumar A, Panda S. A hybrid shuffled frog-leaping and pattern search algorithm for load frequency controller design of a two-area system composing of PV grid and thermal generator. Int J Numer Modell: Electron Netw Dev Field 2020;33. https://doi.org/10.1002/jnm.2694.
[44] Guha D, Roy PK, Banerjee S. Load frequency control of interconnected power system using grey Wolf optimization. Swarm Evol Comput 2016;27:97–115. https://doi.org/10.1016/j.swevo.2015.10.004.
[45] O. Can, A. Ozturk, H. Eroğlu, H. Kotb, A novel Grey Wolf optimizer based load frequency controller for renewable energy sources integrated thermal power systems, Electr Power Compon Syst 49 (2022) 1248–59. https://doi.org/10.1080/15325008.2022.2050450.
[46] Amiri F, Hatami A. Load frequency control for two-area hybrid microgrids using model predictive control optimized by grey wolf-pattern search algorithm. Soft Comput 2023;27:18227–43. https://doi.org/10.1007/s00500-023-08077-0.
[47] Kumar R, Sharma VK. Whale optimization controller for load frequency control of a two-area multi-source deregulated power system. Int J Fuzzy Syst 2020;22:122–37. https://doi.org/10.1007/s40815-019-00761-4.
[48] Can Ö, Eroğlu H, Öztürk A. Automatic generation controller based on whale optimization algorithm in PV-thermal power systems. J Facult Eng Architect Gazi Univer 2023;38:915–26. https://doi.org/10.17341/gazimmfd.984019.
[49] Irudayaraj AXR, Wahab NIA, Premkumar M, Radzi MAM, Bin Sulaiman N, Veerasamy V, Farade RA, Islam MZ. Renewable sources-based automatic load frequency control of interconnected systems using chaotic atom search optimization[Formula presented]. Appl Soft Comput 2022;119. https://doi.org/10.1016/j.asoc.2022.108574.
[50] Ekinci S, Can O, Ayas MS, Izci D, Salman M, Rashdan M. Automatic generation control of a hybrid PV-reheat thermal power system using RIME algorithm. IEEE Access 2024;12:26919–30. https://doi.org/10.1109/ACCESS.2024.3367011.
[51] Vijaya Chandrakala KRM, Balamurugan S. Simulated annealing based optimal frequency and terminal voltage control of multi source multi area system. Int J Electr Power Energy Syst 2016;78:823–9. https://doi.org/10.1016/j.ijepes.2015.12.026.
[52] Ghasemi M, Golalipour K, Zare M, Mirjalili S, Trojovský P, Abualigah L, Hemmati R. Flood algorithm (FLA): an efficient inspired meta-heuristic for engineering optimization. J Supercomput 2024. https://doi.org/10.1007/s11227-024-06291-7.

[53] Katipoğlu D, Soylu S. Design of optimal FOPI controller for two-area time-delayed load frequency control system with demand response. J Electr Eng Technol 2024. https://doi.org/10.1007/s42835-024-01900-0.
[54] Khadanga RK, Kumar A, Panda S. A novel modified whale optimization algorithm for load frequency controller design of a two-area power system composing of PV grid and thermal generator. Neur Comput Appl 2020;32:8205–16. https://doi.org/10.1007/s00521-019-04321-7.
[55] Ibrahim AM, Tawhid MA. IGA: an improved genetic algorithm for real-optimization problem. In: Dey N, editor. Applied genetic algorithm and its variants: case studies and new developments. Singapore: Springer Nature Singapore; 2023. p. 105–38. https://doi.org/10.1007/978-981-99-3428-7_5.